

Effect of Ligand Electronics on the Stability and Chain Transfer Rates of Substituted Pd(II) α -Diimine Catalysts¹

Chris S. Popeney and Zhibin Guan*

Department of Chemistry, University of California, 1102 Natural Sciences 2, Irvine, California 92697

Received January 28, 2010; Revised Manuscript Received March 30, 2010

ABSTRACT: The effect of electron-donating and -withdrawing groups on the ligands of Pd(II) α -diimine olefin polymerization catalysts on catalyst stability, activity, and polymer molecular weight is investigated. The polyethylene molecular weight and the productivity of catalysts bearing substituted bis(aryl)dimethyldiazabutadiene (Me₂DAB) and bis(aryl)acenaphthenequinonediimine (BIAN) ligands were analyzed over time at room temperature and 40 °C to monitor catalyst stability and chain transfer processes. The introduction of electron-donating groups led to a dramatic increase in polymer molecular weight, with polymer chains still growing after 24 h of polymerization. The amino-substituted Me₂DAB analogue afforded polymer of more than twice the molecular weight compared to the polymer made with the unsubstituted analogue after 24 h of polymerization. The unsubstituted catalysts and those bearing electron-withdrawing groups, however, reached a maximal molecular weight, generally lower, after a comparatively short time, which was presumably due to higher chain transfer rates. Electron-donating groups also provided increased stability to the catalysts leading to longer catalyst lifetimes. Both of these effects are likely due to stabilization of the reactive, electron-deficient, and coordinatively unsaturated alkyl agostic intermediate, the reactivity of which is key to both chain transfer and decomposition processes.

Introduction

Since the discovery of cationic Ni(II) and Pd(II) catalysts 15 years ago,² the development of late-transition-metal catalysts for the polymerization of olefins has been spurred by their high functional group tolerance and their ability to incorporate useful comonomers.^{2–9} These systems, the cationic Ni(II) and Pd(II) α -diimine catalysts in particular, have also become especially attractive due to their ability to afford novel branched polymers in a controllable manner. While research in neutral Ni(II) and Pd(II) catalysts has recently taken off due to further improvements on functional group tolerance and thermal stability,^{10–15} the original cationic Ni(II) and Pd(II) α -diimine catalysts are the subjects of a large body of work. The Pd(II) catalysts are particularly well-studied because of their unique ability to introduce chain branching, giving rise to varied polymer architectures that have made them subjects of numerous mechanistic investigations.^{6,16–20} Because of this ability to control polymer topology and the aforementioned tolerance of polar olefins, the Pd(II) α -diimine catalysts have been employed in the construction of complex polymeric structures in a simple, one-pot syntheses.^{9,21,22}

Despite these special attributes, these catalysts suffer from relatively low thermal stability, as evidenced by their rapid decomposition and drastically reduced polymer molecular weight at temperatures above 50 °C.¹⁶ Furthermore, polymerization under low olefin concentrations or in the presence of polar comonomers leads to greatly reduced catalytic activities. The combination of low thermal stability and activity at desired conditions hinders further development of this family of catalysts and advocates the need to develop improved catalyst systems.

Previous research on Pd(II) α -diimine catalyst performance has focused primarily on ligand structure as opposed to ligand

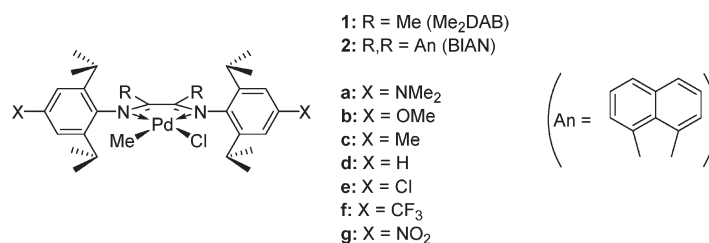
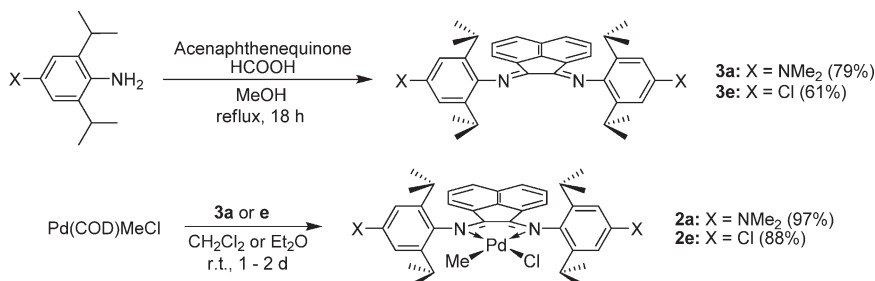
electronics, which are widely known to play a substantial role in various organometallic reactions.^{23–25} Recent reports have described the placement of substituents onto α -diimine ligands and their effect on the σ -donating ability to Pd(II) and thus the Lewis acidity of the metal.^{26,27} In response, we carried out an investigation of the polymerization behavior of a series of Pd(II) α -diimine catalysts bearing substituents in the *para*-aryl position on the ligand aromatic rings.²⁸ We discovered that this substitution was able to perturb the metal electronics in a regular manner, as evidenced by the remarkably linear correlation observed in the stretching frequencies of the corresponding carbonyl complexes. Furthermore, several trends were observed in the physical properties of the resulting polymers. The introduction of substituents of increasing electron-donating ability led to catalysts that afforded polymers of higher molecular weight, slightly reduced branching density, and a corresponding shift toward less dendritic polymer topologies. In the case of copolymerizations with methyl acrylate, a clear and pronounced trend of increasing acrylate incorporation ratio and overall tolerance to polar functionality was also observed over the range of substitution explored.

In contrast to the significant trends previously described, the effect of substitution on other catalytic properties such as activity and thermal stability were difficult to discern with the data then available.²⁸ Since then, more detailed experiments have been performed on the substituted α -diimine complexes of types **1** and **2** (Chart 1) which we now describe herein. Particular emphasis of the new study was placed on the elucidation of trends in catalyst thermal stability through careful observation of polymerization over time. Further analysis on the dependence of polymer molecular weight (MW) on substitution will also be presented.

Results

The Pd(II) complexes **1a–g** bearing α -diimine ligands with backbone methyl substituents, the bis(aryl)dimethyldiazabutadiene

*Corresponding author. E-mail: zguan@uci.edu.

Chart 1. Aryl-Substituted Pd(II) α -Diimine ComplexesScheme 1. Synthesis of Diimines **3a** and **3e** and Pd(II) Complexes **2a** and **2e**Table 1. Properties of Polyethylene Produced at 22 °C^a

entry	catalyst	M_n (kg/mol) ^b		M_w/M_n ^c	R_g (nm) ^d	B^e	catalyst lifetime (h) ^f
		3 h	24 h				
1	1a	220	627	1.25	27.2 ± 1.1	95.5	>24
2	1b	192	433	1.31	23.2 ± 2.1	95.9	24
3	1c	193	425	1.34	23.0 ± 2.5	95.3	24
4	1d	225	253	1.15	15.1 ± 4.1	95.2	>24
5	1e	241	261	1.17	14.2 ± 4.1	96.7	12
6	1f	332	400	1.18	20.3 ± 4.7	96.7	6
7	1g	170	178	1.50	13.9 ± 3.5	100.3	3
8	2a	39.4	70.4	1.28	10.0 ± 6.8	103.9	>24
9	2d	32.8	43.5	1.31	N/A ^g	103.8	>24
10	2e	30.4	34.0	1.37	N/A ^g	106.3	>24

^a Initial polymerization conditions: 5.0 μ mol of catalyst and 1.5 equiv of NaBAF in 25 mL of 3:1 toluene/chlorobenzene, 1 atm of ethylene pressure. Aliquots of 5 mL of the polymerization mixture were taken at 3, 6, and 12 h, and the remaining mixture was collected at 24 h. ^b Number-averaged molecular weight at 3 and 24 h aliquots obtained from SEC-MALLS. ^c Polydispersity obtained from SEC-MALLS for 24 h aliquots. ^d Radius of gyration obtained from MALLS for 24 h aliquots. ^e Polymer branching density per 1000 carbons obtained from ¹H NMR for 24 h aliquots. ^f Catalyst lifetimes estimated from Figure 1. ^g R_g too small for accurate measurement by MALLS.

(Me₂DAB) ligands, and a series of aryl substituents ranging from strongly donating amino to withdrawing nitro groups have been described previously.²⁸ Since we frequently work with catalysts derived from α -diimine ligands bearing the aromatic bis-(aryl)acenaphthenequinonediimine (BIAN) backbone, we also prepared in this study two new substituted BIAN analogues **2a** and **2e**, bearing amino and chloro substitution, respectively, to accompany the existing unsubstituted complex **2d**. The BIAN ligands **3a** and **3e** were prepared by condensation of acenaphthenequinone with the appropriate substituted aniline in methanol and catalytic formic acid (Scheme 1).²⁹ The corresponding Pd(II) complexes were then prepared by displacement of 1,5-cyclooctadiene (COD) from the precursor Pd(COD)MeCl.³⁰

Polymerizations were carried out at 1 atm of ethylene pressure in toluene–chlorobenzene mixtures by direct *in situ* activation of the methyl chlorides **1a–g** and **2a,d,e** by the addition of an excess of sodium tetrakis(3,5-bis(trifluoromethyl)phenyl)borate (NaBAF) to solutions of the complexes.³¹ To accurately monitor catalyst activity, thermal stability, and polymer chain growth, aliquots of known volume were periodically taken from the polymerization

Table 2. Properties of Polyethylene Produced at 40 °C^a

entry	catalyst	M_n (kg/mol) ^b		M_w/M_n ^c	R_g (nm) ^d	B^e	catalyst lifetime (h) ^f
		3 h	24 h				
1	1a	231	234	1.39	18.9 ± 3.8	94.4	6
2	1b	246	275	1.33	19.5 ± 2.7	96.8	12
3	1c	255	271	1.36	19.1 ± 2.3	95.8	12
4	1d	230	252	1.37	19.0 ± 2.5	94.6	6
5	1e	249	256	1.32	18.8 ± 1.9	97.3	3
6	1f	195	195	1.28	13.9 ± 3.8	97.1	3
7	2a	24.6	24.2	1.27	N/A ^g	104.1	6
8	2d	19.1	19.3	1.24	N/A ^g	107.1	24
9	2e	17.0	19.6	1.21	N/A ^g	106.7	12

^a Initial polymerization conditions: 5.0 μ mol of catalyst and 1.5 equiv of NaBAF in 25 mL of 3:1 toluene/chlorobenzene, 1 atm of ethylene pressure. Aliquots of 5 mL of the polymerization mixture were taken at 3, 6, and 12 h, and the remaining mixture was collected at 24 h. ^b Number-averaged molecular weight at 3 and 24 h aliquots obtained from SEC-MALLS. ^c Polydispersity obtained from SEC-MALLS for 24 h aliquots. ^d Radius of gyration obtained from MALLS for 24 h aliquots. ^e Polymer branching density per 1000 carbons obtained from ¹H NMR for 24 h aliquots. ^f Catalyst lifetimes estimated from Figure 2. ^g R_g too small for accurate measurement by MALLS.

mixtures. Catalyst productivities were determined by measurement of polymer yield, and polymer properties were then determined as a function of time to examine the time-dependent behavior of the catalysts. Details of the polymerizations can be found in Tables 1 and 2.

Catalyst Thermal Stability. The results of the catalyst activity and stability analysis at room temperature (22 °C) for catalysts **1a–g** bearing the Me₂DAB series ligands are shown in Figure 1a as a collection of catalyst productivity, in terms of polymer mass per mole of catalyst, versus time profiles. The trends in catalyst activity and stability over the ligand substitution series were complicated by the existence of substituent-specific effects. As previously reported,²⁸ the nitro-substituted catalyst **1g** was deactivated almost immediately after the initiation of polymerization. This instability might be attributed to a side reaction facilitated by the nitro group involving prompt reduction of Pd(II) to palladium black, which could be seen in the reaction mixture after a short time. The dimethylamino-substituted catalyst **1a** and unsubstituted catalyst **1d** were the most active and

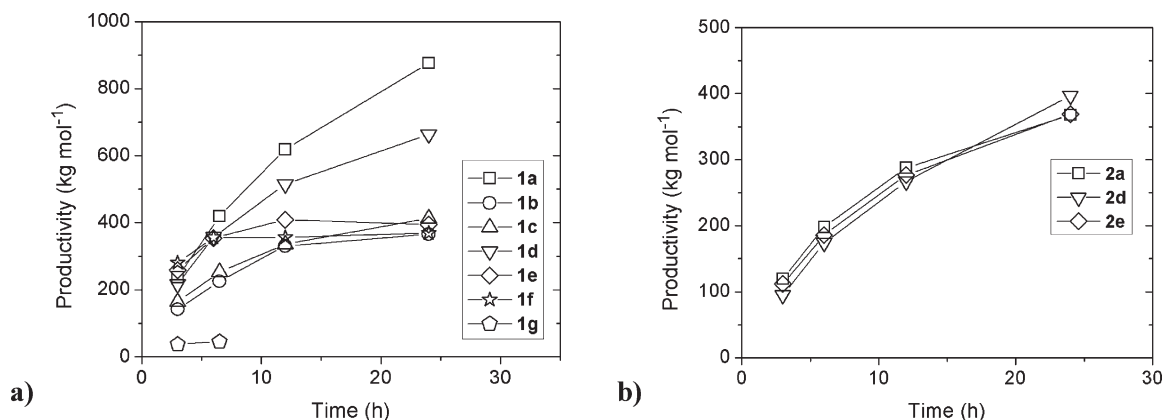


Figure 1. Plots of catalyst productivity vs time at 22 °C for (a) Me₂DAB series catalysts **1a–g** and (b) BIAN series catalysts **2a,d,e**.

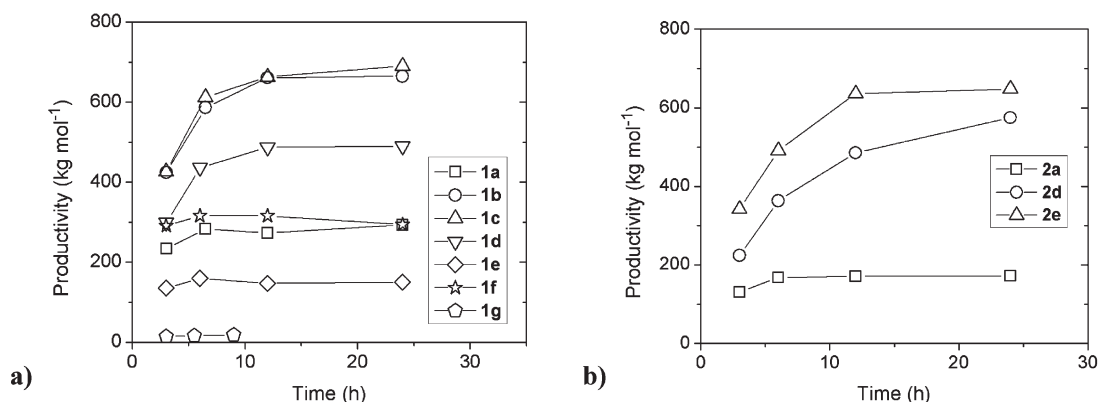


Figure 2. Plots of catalyst productivity vs time at 40 °C for (a) Me₂DAB series catalysts **1a–g** and (b) BIAN series catalysts **2a,d,e**.

stable at room temperature, exhibiting productivities that were still increasing after 24 h. Among the other catalysts, Cl- and CF₃-substituted catalysts **1e,f** showed high activity initially but appeared to undergo complete deactivation within 6–10 h while catalysts **1b,c** were still active after 24 h. Thus, the following stability trend can be summarized for substituted Me₂DAB catalysts at room temperature: NO₂ ≪ CF₃ ~ Cl < Me ~ OMe < H ~ NMe₂. The BIAN-based catalysts (Figure 1b) were found to be roughly half as active at room temperature as the Me₂DAB-based catalysts, in agreement with published reports of ethylene homopolymerizations.⁴ All three BIAN catalysts **2a,d,e** gave results comparable to one another and appeared to have higher stability in general than the Me₂DAB-based systems. For clarity, tables of the actual productivities are given in Table S1 of the Supporting Information.

The sensitivity of the catalysts to temperature was investigated by conducting analogous experiments at 40 °C. The low thermal stability of NMe₂-substituted catalyst **1a** at 40 °C was particularly striking. The reasons for the rapid deactivation of **1a** at elevated temperature are unclear, although it will be seen that this is a general phenomenon for amino-substituted catalysts. Otherwise, the same trend in stability was observed. On the basis of the data shown in Figure 2a and with the amino catalyst excluded, the following trend of stability at 40 °C can be generalized for the Me₂DAB series catalysts: NO₂ ≪ CF₃ ~ Cl < H ~ Me ~ OMe. Most of the Me₂DAB series of catalysts appear to be deactivated after ~10 h of polymerization, and none of them remained active after 24 h of polymerization at 40 °C. The high productivity seen after short polymerization times is evidence of initial activities that are higher than at room temperature, although only the most stable catalysts **1b** and

1c were stable for long enough to have higher overall productivities after a 24 h polymerization period. Among the BIAN series catalysts (Figure 2b), catalyst **2a**, like **1a**, deactivated quickly at 40 °C, presumably by the same process. On the other hand, **2d** and **2e** exhibited higher thermal stability compared to their Me₂DAB analogues. For example, catalyst **2e** was significantly more stable than **1e**, an effect that likely resulted from the rigidity of the planar acenaphthyl backbone (see below). The productivities are tabulated in Table S2 of the Supporting Information.

The measurement of productivity after short reaction times permitted the analysis, although with limited accuracy, of intrinsic catalyst activity. At 22 °C, the Me₂DAB series catalysts exhibited turnover numbers after 3 h that varied by as much as a factor of 2 (Figure 1a) if NO₂-substituted **1g** is excluded. The electron-deficient catalysts **1e** and **1f** seemed more active than the electron-rich analogues **1b** and **1c**. The CF₃-substituted catalyst **1f** appeared to have the highest initial activity at 22 °C, which was further supported by the high polymer MW afforded by the catalyst after short reaction times (see below). Curiously, substitution had little effect on the apparent catalyst activity of the three BIAN catalysts until the temperature was increased to 40 °C, upon which a similar trend could be seen. For the Me₂DAB series at higher temperatures the opposite trend was observed: the electron-rich catalysts (aside from amino-substituted **1a**) exhibited higher activities. This effect, contrary to what was seen at room temperature, probably stemmed from the low thermal stabilities of the electron-poor catalysts and their appreciable decomposition at 40 °C after only 3 h, leading to a detrimental effect on catalyst productivity. Because the observed productivity is dependent on both the inherent

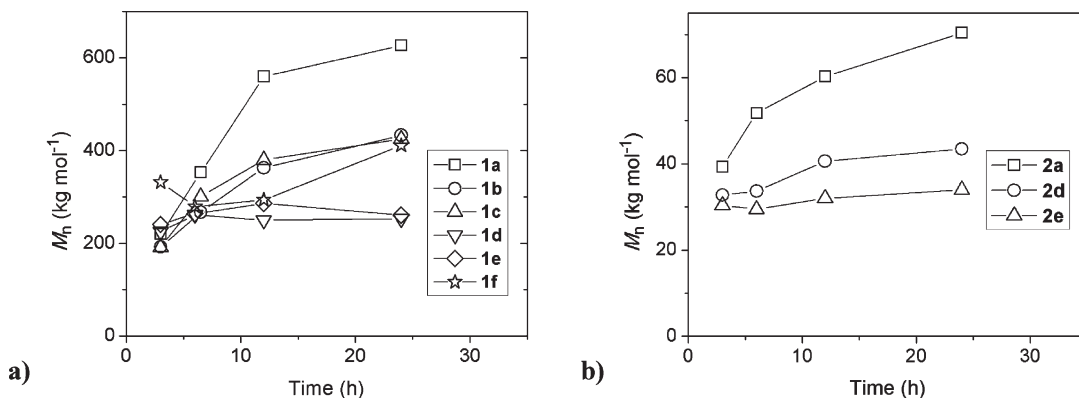


Figure 3. Plots of number-averaged MW vs time at 22 °C for (a) Me₂DAB series catalysts **1a–g** and (b) BIAN series catalysts **2a,d,e**.

activity and stability of the catalysts, it is difficult to deconvolute and separately analyze the two individual properties from the current experimental data.

Polymer Molecular Weight. The MW of polyethylene obtained by the catalysts in the polymerizations above was measured by multiangle laser light scattering (MALLS) analysis after separation by gel permeation chromatography (GPC). A significant dependence on substituent was observed in the data with an overall trend of higher MW polymer produced from catalysts bearing more electron-donating ligands. As shown in Table 1, polymers of high number-averaged molecular weight (M_n) were produced with the electron-rich Me₂DAB catalysts **1a–c** (entries 1–3). Catalyst **1a** afforded polymer of more than double the M_n of the unsubstituted catalyst **1d** (entry 4) after a polymerization period of 24 h at room temperature. The BIAN catalysts afforded lower MW polymer than the Me₂DAB catalysts because of an increased rate of chain transfer (entries 8–10), which is in agreement with previous studies,^{6,16} although the same trend was evident. The M_n of polymer produced by **2a** was nearly twice that of catalyst **2d** after 24 h of polymerization. Polymer chain growth behavior at 22 °C can be seen in the MW vs time profiles in Figure 3. Further discussion of polymer MW can be found in the following section.

At 40 °C, M_n peaked early during polymerizations with all the catalysts as a result of increased chain transfer and catalyst decomposition rates (Table 2). Overall, there was less influence from the *para*-aryl substituents at this temperature, and the α -diimine backbone substituent instead became the most dominant structural feature controlling MW. Although both chain transfer and deactivation processes were expected to become more prevalent at higher temperature, catalyst deactivation was likely more significant among Me₂DAB catalysts than BIAN catalysts due to the lower stability of the former.

Discussion

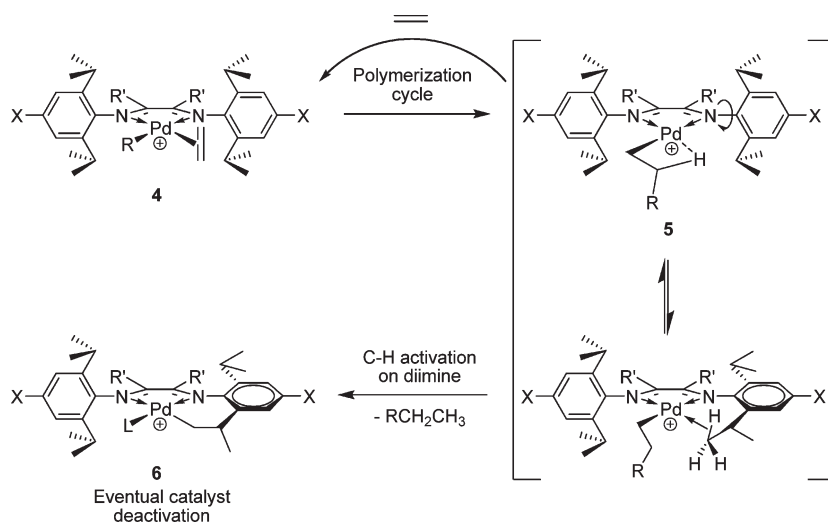
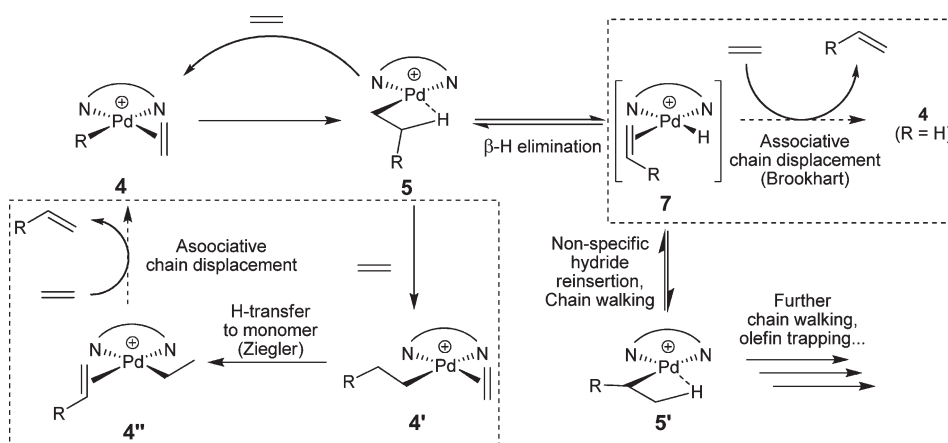
Results from these polymerization experiments lend further support to the previously identified role of ligand electronics on catalyst stability. The presence of electron-donating groups on the α -diimine ligands has an overall stabilizing effect on the catalysts and slows the rate of deactivation processes (with exception of the dimethylamino-substituted catalyst at high temperatures). Although the decomposition pathways are still not well understood, detailed mechanistic studies by Brookhart have detected the products of C–H activation of the ligand with coordinatively unsaturated Pd(II) intermediates.¹⁶ This intermediate is most likely alkyl agostic complex **5**, which forms after migratory insertion of bound olefin in alkyl olefin complex **4**

(Scheme 2). This highly electrophilic agostic complex is presumed to undergo C–H activation of the diimine isopropyl groups in the 2,6-aryl positions, affording palladacycle **6**. Electron-donating α -diimine ligands could stabilize intermediate **5** by making the metal center less reactive toward C–H activation. Intuitively, this process should become more favorable as metal electrophilicity increases.

In the literature, the reported electronic effects on C–H activation reactivity are complex and seem case dependent.^{23,32,33} It is thus difficult to rationalize the trends regarding electronic effects on the stability of Pd(II) α -diimine polymerization catalysts based on existing examples. It is known that ligand steric effects play a significant role in complex stability. For example, catalysts with smaller 2,6-dimethyl groups on the aryl rings are known to show increased stability compared to the isopropyl-substituted analogues described herein because access of the smaller 2,6-dimethyl groups to the metal is restricted.¹⁶ The rigidity of the diimine backbone also imparts a positive effect on stability for this reason,³⁴ at least partly explaining the higher stabilities of the BIAN series complexes when compared to the Me₂DAB complexes. From these observations, it is possible that the substitution of electron-donating groups could decrease the favorability of C–H activation by perturbing the ligand geometry to limit the close approach of the metal to the ligand axial alkyl moieties. It has been observed in α -diimine complexes, however, that the Pd–N coordination strength has little influence on metal–ligand bond lengths,³⁵ likely resulting in little change in complex geometry as substituents are introduced. Finally, electron-deficient α -diimine ligands should be more prone to decomplexation, which could provide an additional route to catalyst decomposition. To the best of our knowledge, this route of deactivation has not been explored.

The ultimately reachable polymer MW is dependent on three distinct processes, in which polymer chain growth (catalyst activity) is offset by the negative effects of chain transfer and catalyst decomposition. The relative importance of each of these rates on MW control can be determined for each catalyst from the above thermal stability and MW data. The stabilities of all the catalysts can be estimated from the approximate time of complete catalyst deactivation and is shown in Tables 1 and 2 as “catalyst lifetime”. In the first case, catalysts **1d**, **2d**, and **2e** (Table 1, entries 4, 9, and 10), although quite stable at 22 °C, nevertheless exhibited little increase in M_n after an initial period of polymer growth. Chain transfer was thus concluded to be an important chain termination process leading to maximal MW after short reaction times. On the other hand, catalyst deactivation can be concluded as being significant among the less robust electron-deficient catalysts **1e–g** (Table 1, entries 5–7) in addition to chain transfer. Nitro-substituted catalyst **1g** represents an extreme example in which decomposition occurred completely

Scheme 2. Catalyst Decomposition via C–H Activation of Agostic Complex 5

Scheme 3. Possible Chain Transfer Pathways in Pd(II) α -Diimine-Catalyzed Polymerization

during the initial rapid chain growth phase, leading to small amounts of low-MW polymer of high polydispersity. Although chain growth with CF_3 -substituted catalyst **1f** was also of short duration, it produced polymers of the highest MW for 3 h polymerization time. This suggests that the intrinsic activity of the catalyst was higher than that of the others and able to offset the higher chain transfer or decomposition rates. Similar activity enhancement appeared to take place with chloro-substituted **1e** as well, albeit to a lesser extent. Lastly, catalysts **1a–c** and **2a** were not only stable over the course of the polymerization runs but also afforded polymers of steadily increasing M_n during that time (Table 1, entries 1–3 and 8, and Figure 3). These electron-rich catalysts exhibited both low chain transfer and low catalyst decomposition rates, thereby giving polymers of high MW after sufficient polymerization time.

The positive effect on polymer molecular weight from the presence of an electron-rich α -diimine ligand can be attributed to two effects. First, the stability of the catalyst itself is increased, which allows for a longer active polymerization time. In addition, the chain transfer rate is appreciably reduced, resulting in a longer residence time of a single polymer chain on the metal. The means by which substitution affects the chain transfer rate remains unclear, although some insight can be gained by examination of the polymerization mechanism, represented in Scheme 3. The two most important species in the catalytic cycle are the alkyl olefin complex **4**, the catalyst resting state, and the coordinatively unsaturated alkyl agostic insertion product **5**. The alkyl agostic

complex can undergo a wide range of transformations, including β -hydride elimination to olefin hydride complex **7**. As proposed by Brookhart and co-workers,^{4,5,16} chain transfer in the Pd(II) α -diimine system proceeds by an associative mechanism by which the axial approach of ethylene displaces the growing polymer chain.^{16–18} A more strongly electron-donating ligand could stabilize the electron-deficient agostic complex **5** and reduce the rate of β -hydride elimination and formation of **7** and subsequent chain transfer. In fact, a small decrease in the polymer branching density B (branches per 1000 carbons, Tables 1 and 2) of about 5% from electron-deficient catalyst **1g** to **1a** supports this hypothesis, since the chain walking mechanism responsible for branching requires the formation of olefin hydride complexes like **7**. In addition, a more strongly electron-donating ligand could stabilize the cationic intermediates such as **4** and **7**, making the coordination of the incoming ethylene more difficult. In other words, the d_{z^2} orbital of the Pd(II) is pushed to higher energy by a more strongly donating ligand, decreasing its tendency to coordinate incoming ethylene.

Computational studies by Morokuma and co-workers have suggested that the barrier to hydride reinsertion in complex **7** is extremely low (less than 1 kcal/mol), and thus this intermediate exists only briefly.^{36,37} Further theoretical calculations by Ziegler and co-workers have proposed that the alkyl ethylene complexes **4** themselves may be prone to chain transfer by a concerted hydride shift from polymer chain to bound ethylene (alkyl olefin complexes **4**, **4'**, and **4''** are all capable of undergoing chain

transfer as long as the alkyl group contains a β -hydrogen).^{38,39} Since these computational models also predict a transition state geometry with ligands in the axial sites, electronic changes to the ligands should affect this mechanism in a manner similar to the more traditional associative chain transfer mechanism discussed above. Because neither proposed mechanism has been disproved, both remain potential routes for chain transfer in the Pd(II) α -diimine polymerization system and deserve consideration.

Conclusions

A series of Pd(II) α -diimine polymerization catalysts possessing a range of electron-donating and -withdrawing groups were examined to probe the effects of substitution on catalyst activity, thermal stability, and polymer chain growth. The polymer yield and polymer molecular weight were analyzed at fixed time increments during polymerization to monitor the catalytic behavior and obtain insight on the relative importance of chain transfer and catalyst decomposition. Several catalysts bearing substituted Me₂DAB ligands bearing dimethyl backbones and a few BIAN-type catalysts with rigid aromatic backbones were studied.

Limited information was obtained regarding intrinsic catalyst activity that indicated an increase in activity with more electron-withdrawing substituents. A far clearer trend was observed in catalyst stability, in which catalysts bearing electron-donating groups underwent deactivation far more slowly than their electron-deficient analogues. The amino-substituted catalysts did not follow these trends at higher temperatures, becoming dramatically less stable under such conditions for unknown reasons. Overall, the increased stability of the electron-rich catalysts likely results from stabilization of the reactive electrophilic and coordinatively unsaturated alkyl agostic intermediates.

A pronounced dependence of polymer MW on the ligand electronic properties was also observed. Catalysts bearing stronger electron-donating groups were able to produce polymer of increasing M_n at prolonged reaction time. Therefore, it was concluded that these catalysts are in fact more resistant to chain transfer than the unsubstituted catalysts or analogues bearing electron-withdrawing groups. Presumably, the stronger electron-donating character of the ligands of these catalysts stabilizes the alkyl agostic catalytic intermediate, inhibiting β -hydride elimination and subsequent chain transfer.

Experimental Section

General Considerations. All catalyst handling was carried out in a Vacuum Atmospheres glovebox filled with nitrogen. All other moisture and air-sensitive reactions were carried out in flame-dried glassware using magnetic stirring under a positive pressure of argon or nitrogen. Removal of organic solvents was accomplished by rotary evaporation and is referred to as concentrated *in vacuo*. Flash column chromatography was performed using forced flow on EM Science 230–400 mesh silica gel. NMR spectra were recorded on Bruker DRX400 and DRX500 FT-NMR instruments. Proton and carbon NMR spectra were recorded in ppm and were referenced to indicated solvents at indicated temperature, if different than ambient. Data were reported as follows: chemical shift, multiplicity (s = singlet, d = doublet, t = triplet, q = quartet), integration, and coupling constant(s) in hertz (Hz). Multiplets (m) were reported over the range (ppm) at which they appear at the indicated field strength. Elemental analysis (for new compounds) was performed by Atlantic Microlab, Norcross, GA.

Materials. Toluene, tetrahydrofuran (THF), diethyl ether, and dichloromethane were purified by passing through solvent purification columns following the method introduced by Grubbs and are referred to as dry.⁴⁰ Unless otherwise stated, all solvents and reagents were purchased from commercial suppliers and used as received. Unsubstituted ligands and Pd

complexes,^{4,5} 2,6-diisopropyl-4-(dimethylamino)aniline,⁴¹ 4-chloro-2,6-diisopropylaniline and all substituted Me₂DAB series ligands and Pd complexes,²⁸ Pd(COD)MeCl,⁴² and sodium tetrakis(3,5-bis(trifluoromethyl)phenyl)borate⁴³ (NaBAF) were prepared by known literature procedures. Chlorobenzene (Aldrich, anhydrous) was used as received.

ArN=C(An)-C(An)=NAr, Ar \equiv 2,6-*i*Pr₂-4-NMe₂C₆H₂(N^{Me}₂NN^{An}, **3a**). To a suspension of 2,6-diisopropyl-4-(dimethylamino)aniline (1.497 g, 6.79 mmol) and acenaphthenequinone (0.557 g, 3.056 mmol) in 20 mL of methanol was added 0.5 mL of formic acid. The mixture was heated to reflux with stirring for 4 h, cooled, and filtered. The solid was washed with cold methanol and dried *in vacuo* to afford **3a** as a purple solid (1.566 g, 79%). ¹H NMR (500 MHz, CDCl₃): δ 0.95 (d, 12H, J = 6.8 Hz), 1.22 (d, 12H, J = 6.7 Hz), 2.90–3.15 (m, 16H), 6.72 (s, 4H), 6.78 (d, 2H, J = 7.2 Hz), 7.36 (t, 2H, J = 7.6 Hz), 7.84 (d, 2H, J = 8.2 Hz). ¹³C NMR (125 MHz, CDCl₃): δ 23.41, 23.57, 29.0, 41.6, 109.0, 123.4, 128.02, 128.63, 129.98, 131.26, 136.4, 139.40, 140.76, 148.3, 162.1. HR-MS calcd for [C₄₀H₅₀N₄ + H]⁺: 587.4114. Found: 587.4127.

ArN=C(An)-C(An)=NAr, Ar \equiv 2,6-*i*Pr₂-4-ClC₆H₂(^C1NN^{An}, **3e**). To a suspension of 4-chloro-2,6-diisopropylaniline (2.34 g, 11.1 mmol) and acenaphthenequinone (0.906 g, 4.97 mmol) in 30 mL of methanol was added 1.0 mL of formic acid. The mixture was allowed to stir at room temperature overnight and was filtered, and the solid was washed with cold methanol. The solid was recrystallized in 10:1 ethanol/chloroform and dried *in vacuo* to afford **3e** as an orange solid (1.736 g, 61%). ¹H NMR (500 MHz, CDCl₃): δ 0.96 (d, 12H, J = 6.8 Hz), 1.22 (d, 12H, J = 6.8 Hz), 2.98 (septet, 4H), 6.78 (d, 2H, J = 7.2 Hz), 7.25 (s, 4H), 7.44 (t, 2H, J = 7.6 Hz), 7.93 (d, 2H, J = 8.2 Hz). ¹³C NMR (125 MHz, CDCl₃): δ 23.07, 23.40, 29.0, 123.64, 124.12, 128.24, 129.33, 129.58, 129.97, 131.4, 137.7, 141.1, 146.0, 161.6. HR-MS calcd. for [C₃₆H₃₈N₂Cl₂ + H]⁺: 569.2490. Found: 569.2494.

(^{NMe}₂NN^{An})PdMeCl (2a**)**. To a solution of **3a** (0.880 g, 1.50 mmol) in 40 mL of CH₂Cl₂ was added 398 mg of Pd(COD)MeCl (1.50 mmol), and the solution was stirred for 3 h at room temperature. The mixture was concentrated, and the residue was dried *in vacuo* overnight to afford **2a** as a dark green solid (1.080 g, 97%). ¹H NMR (400 MHz, CDCl₃): δ 0.85 (s, 3H), 0.90 (d, 6H, J = 6.9 Hz), 0.95 (d, 6H, J = 6.9 Hz), 1.37 (d, 6H, J = 6.8 Hz), 1.47 (d, 6H, J = 6.7 Hz), 3.05 (s, 6H), 3.07 (s, 6H), 3.39 (septet, 4H, J = 6.8 Hz), 6.66 (d, 1H, J = 7.2 Hz), 6.70 (s, 2H), 6.71 (s, 2H), 6.87 (d, 1H, J = 7.2 Hz), 7.43 (t, 1H, J = 7.7 Hz), 7.45 (t, 1H, J = 7.7 Hz), 7.97 (d, 1H, J = 8.0 Hz), 8.02 (d, 1H, J = 8.1 Hz). ¹³C (125 MHz, CDCl₃): δ 3.6, 23.38, 23.48, 23.82, 24.10, 28.85, 29.35, 40.79, 40.88, 107.99, 108.15, 124.41, 124.75, 127.00, 127.75, 128.63, 128.79, 130.20, 130.69, 131.23, 132.36, 133.61, 139.15, 140.07, 143.4, 149.74, 150.20, 168.3, 172.7. Anal. Calcd for C₄₁H₅₃N₄ClPd: C, 66.21; H, 7.18; N, 7.53. Found: C, 65.94; H, 7.09; N, 7.30.

(^C1NN^{An})PdMeCl (2e**)**. To a suspension of **3e** (250 mg, 0.439 mmol) in 20 mL of diethyl ether was added 116 mg of Pd(COD)MeCl (0.439 mmol), and the solution was stirred overnight at room temperature. The mixture was filtered, and the solid was washed with cold diethyl ether then dried *in vacuo* overnight to afford **2e** as a red solid (282 mg, 88%) found to contain ~12% of the monochlorinated side product. ¹H NMR (500 MHz, CDCl₃): δ 0.86 (s, 3H), 0.92 (d, 6H, J = 6.9 Hz), 0.97 (d, 6H, J = 6.9 Hz), 1.39 (d, 6H, J = 6.7 Hz), 1.48 (d, 6H, J = 6.8 Hz), 3.29–3.41 (m, 4H), 6.62 (d, 1H, J = 7.3 Hz), 6.82 (d, 1H, J = 7.2 Hz), 7.32 (s, 2H), 7.38 (s, 2H), 7.52 (t, 1H, J = 7.8 Hz), 7.54 (t, 1H, J = 7.8 Hz), 8.09 (d, 1H, J = 8.1 Hz), 8.13 (d, 1H, J = 8.3 Hz). ¹³C (125 MHz, CDCl₃): δ 4.0, 23.29, 23.57, 23.74, 24.14, 29.13, 29.58, 124.53, 124.99, 125.13, 125.21, 126.41, 127.17, 129.13, 129.27, 131.45, 131.63, 131.92, 133.24, 134.22, 139.96, 140.67, 140.76, 141.77, 144.1, 168.1, 172.4. Anal. Calcd for C₃₇H₄₁N₂Cl₃Pd + 0.15 C₃₇H₄₂N₂Cl₂Pd: C, 61.55; H, 5.74; N, 3.88. Found: C, 61.74; H, 5.69; N, 3.87.

In-Situ-Activated Polymerization Procedure. An oven-dried 50 mL two- or three-neck flask fitted with septa and a water-cooled

condenser (for elevated temperature polymerizations) was charged with 10 μmol of Pd(II) complex and 15 μmol of NaBAF under an inert atmosphere. A 3:1 ratio of toluene to chlorobenzene was added to bring the reaction volume to 25 mL. Ethylene was added by slowly bubbling through the reaction mixture to maintain ambient pressure during the course of the polymerization. Temperature was controlled by placement in an external oil bath as needed. After 3, 6, and 12 h, 5.0 mL aliquots of the polymerization mixtures were taken and placed into preweighed vials and dried overnight under soft vacuum at 70 °C. After the withdrawal of each aliquot, the volume of remaining mixture was measured by syringe. After 24 h the leftover mixture (~10 mL) was dried by the same means. The yield of polymer and catalyst turnover number (TON) were calculated from the mass of polymer and the amount of catalyst in each aliquot, as determined from the remaining mixture volume to account for solvent evaporation and/or polymer generation.

SEC-MALLS Characterization of Polymers.^{19,20} All the polymers were characterized by size-exclusion chromatography (SEC) coupled to a multiangle laser light scattering detector (MALLS) for obtaining both polymer MW (M_n and M_w) and R_g . Measurements were made on highly dilute fractions eluting from a SEC consisting of a HP Agilent 1100 solvent delivery system/auto injector with an online solvent degasser, temperature-controlled column compartment, and an Agilent 1100 differential refractometer. A 30 cm column was used (Polymer Laboratories PLgel Mixed C, 5 μm particle size) to separate polymer samples. The mobile phase was THF, and the flow rate was 1.0 mL/min. Both the column and the differential refractometer were held at 35 °C. A 30 μL sample of a 2 mg/mL solution was injected into the column. A Dawn DSP 18-angle light scattering detector (Wyatt Technology, Santa Barbara, CA) was coupled to the SEC to measure both the MW and sizes for each fraction of the polymer eluted from the SEC column. ASTRA 4.7 software from Wyatt Technology was used to acquire data from the 18 scattering angles (detectors) and the differential refractometer and compute M_n and M_w from classical light scattering treatments.

Acknowledgment. We thank the National Science Foundation (Chem-0456719, Chem-0723497, DMR-0703988) for funding. C.P. acknowledges the Allergan Foundation, the UCI Department of Chemistry, and Joan Rowland for financial support.

Supporting Information Available: Tables of catalyst productivities with time. This material is available free of charge via the Internet at <http://pubs.acs.org>.

References and Notes

- (1) This paper has been adapted in part from the following thesis: Popeney, C. S. Ph.D. Dissertation, University of California at Irvine, **2008**.
- (2) Johnson, L. K.; Killian, C. M.; Brookhart, M. *J. Am. Chem. Soc.* **1995**, *117*, 6414–6415.
- (3) Ittel, S. D.; Johnson, L. K.; Brookhart, M. *Chem. Rev.* **2000**, *100*, 1169–1203.
- (4) Gibson, V. C.; Spitzmesser, S. K. *Chem. Rev.* **2003**, *103*, 283–315.
- (5) Johnson, L. K.; Mecking, S.; Brookhart, M. *J. Am. Chem. Soc.* **1996**, *118*, 267–268.
- (6) Mecking, S.; Johnson, L. K.; Wang, L.; Brookhart, M. *J. Am. Chem. Soc.* **1998**, *120*, 888–899.
- (7) Gates, D. P.; Svejda, S. K.; Onate, E.; Killian, C. M.; Johnson, L. K.; White, P. S.; Brookhart, M. *Macromolecules* **2000**, *33*, 2320–2334.
- (8) Kang, M.; Sen, A.; Zakharov, L.; Rheingold, A. L. *J. Am. Chem. Soc.* **2002**, *124*, 12080–12081.
- (9) Chen, G.; Ma, X. S.; Guan, Z. *J. Am. Chem. Soc.* **2003**, *125*, 6697–6704.
- (10) Younkin, T. R.; Connor, E. F.; Henderson, J. I.; Friedrich, S. K.; Grubbs, R. H.; Bansleben, D. A. *Science* **2000**, *287*, 460–462.
- (11) Hicks, F. A.; Brookhart, M. *Organometallics* **2001**, *20*, 3217–3219.
- (12) Drent, E.; van Dijk, R.; van Ginkel, R.; van Oort, B.; Pugh, R. I. *Chem. Commun.* **2002**, 744–745.
- (13) Gottker-Schnetmann, I.; Korthals, B.; Mecking, S. *J. Am. Chem. Soc.* **2006**, *128*, 7708–7709.
- (14) Luo, S.; Vela, J.; Lief, G. R.; Jordan, R. F. *J. Am. Chem. Soc.* **2007**, *129*, 8946–8947.
- (15) Kochi, T.; Noda, S.; Yoshimura, K.; Nozaki, K. *J. Am. Chem. Soc.* **2007**, *129*, 8948–8949.
- (16) Tempel, D. J.; Johnson, L. K.; Huff, R. L.; White, P. S.; Brookhart, M. *J. Am. Chem. Soc.* **2000**, *122*, 6686–6700.
- (17) Shultz, L. H.; Tempel, D. J.; Brookhart, M. *J. Am. Chem. Soc.* **2001**, *123*, 11539–11555.
- (18) Shultz, L. H.; Brookhart, M. *Organometallics* **2001**, *20*, 3975–3982.
- (19) Guan, Z.; Cotts, P. M.; McCord, E. F.; McLain, S. J. *Science* **1999**, *283*, 2059–2062.
- (20) Cotts, P. M.; Guan, Z.; McCord, E.; McLain, S. *Macromolecules* **2000**, *33*, 6945–6952.
- (21) Chen, G.; Guan, Z. *J. Am. Chem. Soc.* **2004**, *126*, 2662–2663.
- (22) Chen, G.; Huynh, D.; Felgner, P. L.; Guan, Z. *J. Am. Chem. Soc.* **2006**, *128*, 4298–4302.
- (23) Zhong, H. A.; Labinger, J. A.; Bercaw, J. E. *J. Am. Chem. Soc.* **2002**, *124*, 1378–1399.
- (24) Lanza, G.; Fragala, I. L.; Marks, T. J. *J. Am. Chem. Soc.* **2000**, *122*, 12764–12777.
- (25) Moore, D. R.; Cheng, M.; Lobkovsky, E. B.; Coates, G. W. *Angew. Chem., Int. Ed.* **2002**, *41*, 2599–2602.
- (26) Gasperini, M.; Ragaini, F.; Cenini, S. *Organometallics* **2002**, *21*, 2950–2957.
- (27) Gasperini, M.; Ragaini, F. *Organometallics* **2004**, *23*, 995–1001.
- (28) Popeney, C.; Guan, Z. *Organometallics* **2005**, *24*, 1145–1155.
- (29) van Asselt, R.; Elsevier, C. J.; Smeets, W. J. J.; Spek, A. L.; Benedix, R. *Rec. Trav. Chim. Pays-Bas* **1994**, *113*, 88–98.
- (30) van Asselt, R.; Elsevier, C. J.; Smeets, W. J. J.; Spek, A. L. *Inorg. Chem.* **1994**, *33*, 1521–1531.
- (31) Schmid, M.; Eberhardt, R.; Klinga, M.; Leskela, M.; Rieger, B. *Organometallics* **2001**, *20*, 2321–2330.
- (32) DeYonker, N. J.; Foley, N. A.; Cundari, T. R.; Gunnoe, T. B.; Petersen, J. L. *Organometallics* **2007**, *26*, 6604–6611.
- (33) Tellers, D. M.; Yung, C. M.; Arndtsen, B. A.; Adamson, D. R.; Bergman, R. G. *J. Am. Chem. Soc.* **2002**, *124*, 1400–1410.
- (34) Liu, F.-S.; Hu, H.-B.; Xu, Y.; Guo, L.-H.; Zai, S.-B.; Song, K.-M.; Gao, H.-Y.; Zhang, L.; Zhu, F.-M.; Wu, Q. *Macromolecules* **2009**, *42*, 7789–7796.
- (35) Gasperini, M.; Ragaini, F.; Gazzola, E.; Caselli, A.; Macchi, P. *Dalton Trans.* **2004**, 3376–3382.
- (36) Musaev, D. G.; Svensson, M.; Morokuma, K.; Stromberg, S.; Zetterberg, K.; Siegbahn, P. E. M. *Organometallics* **1997**, *16*, 1933–1945.
- (37) Froese, R. D. J.; Musaev, D. G.; Morokuma, K. *J. Am. Chem. Soc.* **1998**, *120*, 1581–1587.
- (38) Deng, L.; Margl, P.; Ziegler, T. *J. Am. Chem. Soc.* **1997**, *119*, 1094–1100.
- (39) Deng, L.; Woo, T. K.; Cavallo, L.; Margl, P. M.; Ziegler, T. *J. Am. Chem. Soc.* **1997**, *119*, 6177–6186.
- (40) Pangborn, A. B.; Giardello, M. A.; Grubbs, R. H.; Rosen, R. K.; Timmers, F. J. *Organometallics* **1996**, *15*, 1518–1520.
- (41) Carver, F. J.; Hunter, C. A.; Livingstone, D. J.; McCabe, J. F.; Seward, E. M. *Chem.—Eur. J.* **2002**, *8*, 2848–2859.
- (42) Rulke, R. E.; Ernsting, J. M.; Spek, A. L.; Elsevier, C. J.; Vanleeuwen, P. W. N. M.; Vrieze, K. *Inorg. Chem.* **1993**, *32*, 5769–5778.
- (43) Yakelis, N. A.; Bergman, R. G. *Organometallics* **2005**, *24*, 3579–3581.